HHS Public Access

Author manuscript

Sci Transl Med. Author manuscript; available in PMC 2017 July 17.

Published in final edited form as:

Sci Transl Med. 2016 March 30; 8(332): 332ra44. doi:10.1126/scitranslmed.aad3650.

Neuronal heparan sulfates promote amyloid pathology by modulating brain amyloid-β clearance and aggregation in Alzheimer's disease

Chia-Chen Liu[1], **Na Zhao**[1], **Yu Yamaguchi**[2], **John R. Cirrito**[3], **Takahisa Kanekiyo**[1], **David M. Holtzman**[3], and **Guojun Bu**[1,4,*]

[1]Department of Neuroscience, Mayo Clinic, Jacksonville, FL 32224, USA

[2]Sanford Burnham Prebys Medical Discovery Institute, La Jolla, CA 92037, USA

[3]Department of Neurology, Hope Center for Neurological Disorders, Knight Alzheimer's Disease Research Center, Washington University School of Medicine, St. Louis, MO 63110, USA

[4]Fujian Provincial Key Laboratory of Neurodegenerative Disease and Aging Research, Institute of Neuroscience, College of Medicine, Xiamen University, Xiamen, Fujian, China

Abstract

Accumulation of amyloid-β (Aβ) peptide in the brain is the first critical step in the pathogenesis of Alzheimer's disease (AD). Studies in humans suggest that Aβ clearance from the brain is frequently impaired in late-onset AD. Aβ accumulation leads to the formation of Aβ aggregates which injure synapses and contribute to eventual neurodegeneration. Cell surface heparan sulfates (HS), expressed on all cell types including neurons, have been implicated in several features in the pathogenesis of AD including its co-localization with amyloid plaques and modulatory role in Aβ aggregation. Here, we show that removal of neuronal HS by conditional deletion of the *Ext1* gene, which encodes an essential glycosyltransferase for HS biosynthesis, in postnatal neurons of APP/PS1 mice led to a reduction in both Aβ oligomerization and the deposition of amyloid plaques. *In vivo* microdialysis experiments also detected an accelerated rate of Aβ clearance in the brain interstitial fluid (ISF), suggesting that neuronal HS either inhibited or represented an inefficient pathway for Aβ clearance. Interestingly, we found that the amounts of various HS proteoglycans (HSPGs) were increased in postmortem human brain tissues from AD patients, suggesting that this pathway may contribute directly to amyloid pathogenesis. Our findings have implications for AD pathogenesis and provide insight into therapeutic interventions targeting Aβ-HSPG interactions.

*Correspondence should be addressed to Guojun Bu, Department of Neuroscience, Mayo Clinic, 4500 San Pablo Road, Jacksonville, Florida 32224. bu.guojun@mayo.edu.

Author contributions: C.-C. L., T.K., and G.B. designed and set up the research concept. C.-C.L., N.Z., T.K., and G.B. designed and performed the experiments. J.R.C. guided C.-C.L. to perform *in vivo* Aβ microdialysis experiments. D.M.H., Y.Y., and J.R.C. provided valuable technical and conceptual advice and experimental tools. C.-C.L., T.K., and G.B. wrote the manuscript with critical inputs and edits by co-authors.

Competing interests: DH is on the scientific advisory boards of Genentech, AstraZeneca, Neurophage, and Denali, and has consulted for Eli Lilly, AbbVie, Novartis, Ono Pharma. DH is a cofounder of C2N Diagnostics LLC and has equity in the company. The other authors declare no competing interests.

INTRODUCTION

Alzheimer's disease (AD) is the most common form of dementia in which amyloid plaques and neurofibrillary tangles are the major pathological hallmarks. Mounting evidence suggests that the accumulation and aggregation of amyloid-β (Aβ), the major component of amyloid plaques in the brain is a key initiating event in the pathogenesis of AD (1, 2). Aβ is generated from proteolytic processing of amyloid precursor protein (APP) by β- and γ-secretases (3, 4). Genetic and biochemical studies showed that early-onset forms of AD (<1%) are caused by the inheritance of autosomal-dominant mutations that affect APP processing, leading to increases in Aβ production or the propensity for Aβ to aggregate (5). However, much less is known about the pathological mechanisms that modulate Aβ accumulation in the late-onset forms of AD, which account for more than 99% of cases. The amount of Aβ in the brain represents the net balance of Aβ production and clearance (6). Excess Aβ rapidly aggregates to form oligomers, which have been shown to impair synaptic function and eventual cognitive deficits (7). Aβ has a relatively short half-life in the brain, with ~1-2 hours in mouse interstitial fluid (ISF) and ~8 hours in human cerebrospinal fluid (CSF) (8, 9). Intriguingly, increasing evidence indicates that impaired Aβ clearance is a common prelude to late-onset AD (10). Thus, understanding the factors that regulate Aβ clearance is critical to illuminate the pathogenic pathways of AD and to design effective therapies for treating AD.

Heparan sulfate proteoglycans (HSPGs), consisting of heparan sulfate (HS) chains covalently attached to a specific protein core, are abundant cell surface and extracellular molecules that interact with a spectrum of ligands (11, 12). A critical step in the biosynthesis of HS is the elongation of linear polysaccharides composed of alternating glucuronic acid (GlcA) and N-acetylglucosamine (GlcNAc) catalyzed by the EXT1 family of molecules (13). Studies have shown that the biosynthesis of HS is disrupted upon EXT1 deficiency, indicating that the glycosyltransferase activity associated with EXT1 is indispensable for HS assembly (14, 15). HSPGs are ubiquitously expressed in almost all mammalian cell types, and regulate a wide variety of biological processes, including embryonic development, growth factor signaling, cell proliferation, adhesion and migration, and homeostasis (12, 13). HSPGs are present in senile plaques and cerebral amyloid angiopathy (CAA) (16-19). HSPGs have been shown to bind to Aβ and accelerate its oligomerization and aggregation (20-22). Also, HS mediates cellular Aβ uptake, neurotoxicity and inflammatory responses induced by Aβ (23-25). These findings suggest that HSPGs might play important roles in Aβ metabolism and the pathogenesis of AD.

A recent study reported that overexpression of heparanase reduces the amyloid burden in a mouse model, likely by modulating Aβ deposition (26). Here, using a conditional mouse model deficient in neuronal HS in adult brain, we bypassed the developmental effects of HS and investigated the cell type-specific roles of HS in amyloid pathogenesis. Our findings provide *in vivo* evidence that neuronal HS inhibits brain Aβ clearance and promotes amyloid plaque deposition. Specifically, by using *in vivo* microdialysis to measure the clearance rate of soluble Aβ from the brain ISF, we found that deficiency of HS in neurons facilitated Aβ clearance and reduced Aβ aggregation, resulting in a reduction in amyloid plaque deposition. In addition, we showed that several HSPG species were upregulated in

postmortem human brain tissues from AD patients. Together, our results shed light on the mechanisms by which HSPGs modulate brain Aβ metabolism and deposition and suggest that targeting Aβ-HSPG interactions might be a promising strategy to treat AD.

RESULTS

Neuronal HS deficiency decreases Aβ and ameliorates amyloid pathology in an amyloid mouse model

The amount of Aβ in the brain is a net balance of Aβ production and clearance, thus, it is important to analyze the overall impact of altered HSPG expression on brain Aβ and Aβ pathology. To investigate the *in vivo* role of HSPG in brain Aβ metabolism, we conditionally disrupted the expression of the *Ext1* gene encoding the HS polymerizing enzyme in neurons by crossing $Ext1^{flox/flox}$ mice (27) with alpha calcium/calmodulin-dependent protein kinase II (CaMKII-Cre) mice (28), and then we further bred these mice to the APPswe/PS1ΔE9 (APP/PS1) amyloid mouse (29). The use of CamKII-Cre allowed us to bypass the effects of *Ext1* inactivation on embryonic brain development and to selectively study the role of HSPGs in the forebrain neurons of adult mice, which is one of the most vulnerable brain regions in AD. These mice developed normally without detectable morphological changes in the brain, consistent with previous findings (30). We found that *Ext1* expression was decreased in cortex of knockout mice at 12 months of age, but not in cerebellum where CaMKII-Cre was not active (Fig. S1A). Biochemical analysis showed that HS was significantly reduced in CaMKII-Cre active regions, such as cortex and hippocampus, while its amount was unaltered in cerebellum (Fig. S1B). The residual HS observed likely represents the expression within glial cells or brain vasculature (17, 31, 32). As APP/PS1 mice develop amyloid plaques at 5-6 months of age which continue to increase up to 12 months of age (33), we analyzed the burden of amyloid deposition in these mice at 12 months of age. The brain sections of the compound mutants (APP/PS1; $Ext1^{flox/flox}$; CaMKII-Cre. APP/PS1; n$Ext1^{CKO}$; thereafter) and their littermate controls (APP/PS1) were immunostained using an anti-Aβ antibody (34), and the extent of Aβ deposition in the cortical and hippocampal regions was quantified. Interestingly, the amyloid deposition was dramatically decreased in APP/PS1; n$Ext1^{CKO}$ mice (Fig. 1A). Quantification revealed that Aβ burden in 12-month-old APP/PS1; n$Ext1^{CKO}$ mice was about one third of that in APP/PS1 littermate control mice (Fig. 1A). Previous studies demonstrated that HS and HSPGs co-localize with amyloid plaques, in particular in the core of amyloid deposits and blood vessels (26, 32, 35, 36). We thus examined the association of HS or HSPG core proteins with amyloid plaques in our mouse model. Immunohistochemical staining showed that HS was co-localized with Congo red-positive amyloid plaques in the brain parenchyma and leptomeningeal arteries in APP/PS1 mice with heparinase III treatment abolishing HS immunoreactivity (Fig. S1, C and D). As expected, the association between HS and amyloid plaques was dramatically decreased in APP/PS1; n$Ext1^{CKO}$ mice in the cortex, but was not altered in the brain vessels where CaMKII-Cre is not active (Fig. S1, C and D). Deficiency of neuronal HS side chains did not alter the mRNA expression of HSPG protein backbones, including transmembrane syndecans, glycosylphosphatidyl inositol (GPI)-linked glypicans and extracellular matrix HSPGs (perlecan and agrin) in the brains of APP/PS1; n$Ext1^{CKO}$ mice (Fig. S2). Approximately 20-40% of plaques were positive for glypican-1, syndecan-3

and agrin, whereas the co-localization between perlecan and Aβ was minimal (Fig. S3A). Importantly, we observed a reduction in the percentage of amyloid plaques that were positive for various HSPG subtypes (glypican-1, syndecan-3, and agrin) in the cerebral cortex of APP/PS1; n$Ext1^{CKO}$ mice compared to control mice (Fig. S3A, B). Agrin and perlecan, the major HSPGs in the basement membrane of the cerebral vasculature (35, 37), and syndecan-3 were also co-localized with Aβ in the leptomeningeal arteries of APP/PS1 and APP/PS1; n$Ext1^{CKO}$ mice (Fig. S3C).

To further analyze how HS affects the dynamic pools of Aβ, we fractionated cortical and hippocampal mouse brain tissues into Tris-buffered saline (TBS)-soluble, detergent-soluble (TBSX), and insoluble (guanidine-HCl, GDN) fractions (38), and quantified Aβ by ELISA. Though the majority of Aβ in these mice at 12 months of age was distributed in the amyloid plaques and was fractionated in the detergent insoluble fractions, Aβ40 and Aβ42 in the TBSX soluble fractions were also lower in the brains of APP/PS1; n$Ext1^{CKO}$ mice compared with APP/PS1 controls (P <0.01 in cortex; P <0.05 for Aβ40 and P <0.01 for Aβ42 in hippocampus) (Fig. 1B, C). Consistent with decreased Aβ deposition, the concentrations of insoluble Aβ40 and Aβ42 in the guanidine fractions were very high in the APP/PS1 mice in the cortex and hippocampus and were reduced in both brain regions of APP/PS1; n$Ext1^{CKO}$ mice (Fig. 1D, E; P <0.01). Oligomeric Aβ has been implicated as the deleterious form of Aβ peptide (39), thus we examined the amount of soluble oligomeric Aβ in the TBS soluble fraction using an ELISA specific to oligomeric Aβ (40) in the cortex of these mice. We found that Aβ oligomers were significantly decreased in APP/PS1; n$Ext1^{CKO}$ mice compared to APP/PS1 control mice (Fig. 1F; P <0.01). To investigate whether deficiency of HS affected Aβ oligomerization, we further assessed the ratio of Aβ oligomers versus total Aβ in the TBS-soluble fraction of cortex. To quantify total Aβ, the same antibody used in oligomeric Aβ ELISA was utilized to capture Aβ followed by an antibody that recognizes the middle region of Aβ. Interestingly, the ratio of Aβ oligomers/ total Aβ was significantly reduced in APP/PS1; n$Ext1^{CKO}$ mice (Fig. 1G; P <0.01), indicating a decrease of Aβ oligomerization in APP/PS1; n$Ext1^{CKO}$ mouse brain. This result suggests that neuronal HS may promote Aβ oligomerization.

HSPGs have been shown to promote Aβ aggregation and fibril formation (16, 26, 41). Thus, we next characterized amyloid plaque load in APP/PS1 and APP/PS1; n$Ext1^{CKO}$ mice by staining brain sections with Thioflavin S, a fluorescent dye that binds to amyloid fibrils. Consistent with the Aβ immunostaining pattern, we found that deficiency of neuronal HS led to a significant reduction in fibrillar plaques in the cortex (P <0.01) and hippocampus (P <0.05) of APP/PS1; n$Ext1^{CKO}$ mice compared to APP/PS1 controls (Fig. 1H). Together, our results demonstrate that the deficiency of HS in neurons reduced Aβ accumulation and aggregation, resulting in a decrease in amyloid plaque deposition in APP/PS1; n$Ext1^{CKO}$ mice.

Neuronal HS deficiency decreases neuroinflammation in an amyloid mouse model

Abnormal activation of astrocytes and microglia has been observed in the brains of AD patients and APP transgenic mouse models (42). To examine the extent of astrogliosis in these mice, we immunostained the brain sections with anti-GFAP antibody followed by

quantification. The immunostaining for GFAP clearly demonstrated that activation of astrocytes was suppressed in the brains of APP/PS1; n*Ext1*^{CKO} mice compared with those of APP/PS1 mice at 12 months of age (Fig. 2A-C; P <0.01; Fig. S4). The brain sections were also immunostained with anti-Iba1 antibody to examine the extent of microgliosis. The dystrophic microglial reactivity was more evident in APP/PS1 control mice, in which a stronger intensity and activated morphology of microglia were observed (Fig. 2D-F; P <0.01; Fig. S4). These results indicated that elimination of HS in neurons led to a reduction in plaque-associated microglial activation. Western blot analysis also confirmed that the GFAP amount was significantly decreased in the cortex (P <0.01) and hippocampus (P <0.05) of APP/PS1; n*Ext1*^{CKO} mice (Fig. 2G). Tumor necrosis factor alpha (TNF-α), interleukin-1β (IL-1β) and IL-6 are important proinflammatory mediators involved in the pathogenesis of AD (43). Interestingly, neuronal HS deficiency resulted in a reduction of these proinflammatory cytokines, including TNF-α, IL-1β and IL-6 (Fig. 2H). These findings demonstrate that *Ext1* inactivation in neurons decreased Aβ deposition accompanied by a reduction in neuroinflammation.

Neuronal HS deficiency increases Aβ clearance in the hippocampus of amyloid model mice

To investigate the mechanism underlying the reduction of Aβ pathology, we used *in vivo* microdialysis to dynamically assess ISF Aβ metabolism in the hippocampus of APP/PS1; n*Ext1*^{CKO} mice and APP/PS1 littermates at 3-4 months of age. Soluble Aβ in ISF has been shown to reflect total soluble Aβ in extracellular pools and is significantly correlated with the amount of Aβ that eventually is deposited in the extracellular space of the brain (8, 44, 45). Hippocampal ISF was sampled in APP/PS1; n*Ext1*^{CKO} mice and APP/PS1 littermates for a stable baseline period during which mice were able to freely move throughout the experiment. To understand whether the decrease of Aβ amount in APP/PS1; n*Ext1*^{CKO} mice was the result of altered Aβ clearance from the ISF, we infused a potent γ-secretase inhibitor directly into mice to rapidly block Aβ production, thus allowing sensitive measurement of the elimination rate of Aβ from the ISF (Fig. 3A; Fig. S5A). ISF Aβ40 and Aβ42 concentration gradually decreased in a time-dependent manner after treatment with the γ-secretase inhibitor, with APP/PS1; n*Ext1*^{CKO} mice showing a faster decline compared with control APP/PS1 mice (Fig. 3B; Fig. S5B). The half-life ($t_{1/2}$) of ISF Aβ40 (P <0.01) and Aβ42 (P <0.05) in the hippocampus of APP/PS1; n*Ext1*^{CKO} mice was significantly shorter compared to that of APP/PS1 mice (Fig. 3C; Fig. S5C). These results indicate that elimination of HS in neurons enhanced the clearance of soluble Aβ from the ISF.

To examine whether *Ext1* inactivation in neurons affects APP processing, total APP and APP processing products in both APP/PS1 and APP/PS1; n*Ext1*^{CKO} mice were analyzed. We found that there were no significant differences in the amount of full-length APP, soluble forms of APP (sAPPα and sAPPβ) and C-terminal fragments (CTFs) between APP/PS1 and APP/PS1; n*Ext1*^{CKO} mice at 12 months of age examined by Western blot analysis (Fig. 3D-F), indicating that deficiency of neuronal HS in these mice did not significantly affect APP processing. Given that HS deficiency in neurons led to decreased insoluble Aβ and a substantial reduction in amyloid plaque deposition without affecting APP processing, we also analyzed the mRNA expression of neprilysin, insulin degrading enzyme, matrix

metalloproteinase 2 (MMP2) and MMP9, which are major Aβ degrading enzymes in the brain. The qRT-PCR results showed no significant differences in the mRNA expression of these enzymes between APP/PS1 and APP/PS1; n$Ext1^{CKO}$ mice (Fig. 3G). Together, these results indicate that deficiency of HS in neurons accelerated Aβ clearance without affecting APP processing or the expression of major Aβ-degrading enzymes in amyloid model mice.

Deficiency of neuronal HSPGs increases the formation of cerebral amyloid angiopathy

Given that Aβ clearance was enhanced in the brains of APP/PS1; n$Ext1^{CKO}$ mice, we thus examined whether deficiency of HS in neurons affected cerebral amyloid angiopathy (CAA) formation. Intriguingly, Aβ deposition (including both Aβ40 and Aβ42) in cortical vessels manifested as CAA was increased (P <0.01) in the APP/PS1; n$Ext1^{CKO}$ mice even though the parenchymal amyloid plaques were substantially decreased in these mice compared to APP/PS1 controls (Fig. 4A, B; Fig. S6). Co-staining of α-smooth muscle actin (α-SMA), a marker for vascular smooth muscle cells, and Aβ confirmed that Aβ was deposited in walls of arterioles in CAA (Fig. 4C). Mounting evidence suggests that the entrapment of brain Aβ in the ISF perivascular lymphatic drainage pathway is the main cause of CAA (46). Given that deficiency of neuronal HS increased Aβ clearance and reduced amyloid deposition in the brain parenchyma, relatively more Aβ might be diverted into perivascular drainage pathways for clearance in APP/PS1; n$Ext1^{CKO}$ mice. As several HSPGs have been shown to be expressed by cells of the cerebral vasculature and are involved in the pathogenesis of CAA (17, 36, 47), the increased cerebrovascular amyloid might be attributed to the HSPGs in the cerebral vasculature.

Several classes of HSPGs are increased in human AD brain tissues

Several HSPGs have been shown to co-localize with senile plaques and CAA (31, 48). To examine whether the distributions of different classes of HSPGs are altered in the pathogenesis of AD, we examined the amounts of HSPGs in the temporal cortex of human control (n = 20, average age 85.1 ± 5.7 years old) and AD (n = 20, average age 84.4 ± 5.2 years old) brain tissues (Table S1). We processed the brain tissues into TBS, detergent-soluble (TBSX) and detergent-insoluble (GDN) fractions, and the amounts of syndecans, glypicans, perlecan and agrin were examined by specific ELISAs. We found that syndecan-1 amount was not different between control and AD brain tissues (Fig. 5A). Interestingly, the amounts of syndecan-3 and syndecan-4 in both the detergent-soluble (P <0.01 for syndecan-3; P <0.05 for syndecan-4) and detergent-insoluble fractions (P<0.05 for syndecan-3; P <0.05 for syndecan-4) were significantly increased in human AD brains (Fig. 5B, C). In addition, glypican-3 in the GDN fraction was elevated (P <0.05) in AD brains although there was no change in the TBSX fraction (Fig. 5D). Glypican-1, an abundant glypican in neurons, was trending to an increase in the GDN fractions although this was not significant (Fig. 5E). We next examined the amounts of secreted extracellular matrix HSPGs, including agrin and perlecan in these human brain tissues, and found that the amount of agrin was increased in the GDN fractions of AD brains (Fig. 5F; P <0.01). A previous study showed that a large fraction of the agrin in AD brains is detergent insoluble (49). In our measurements, the amount of agrin in the TBSX fractions was under the detection limit using currently available ELISAs. Finally, perlecan amount was elevated in both detergent soluble (P <0.01) and insoluble fractions (P <0.05) in AD brain tissues (Fig.

5G). Together, these findings demonstrate that a number of HSPGs, distributed abundantly in the insoluble compartments, were significantly increased in human AD brains.

DISCUSSION

The accumulation and deposition of Aβ in the brain has been hypothesized to drive the pathogenic cascades of AD (1, 2). In fact, substantial amyloid buildup is present in AD brains long before the clinical onset of the disease (50, 51). Mounting studies have clearly demonstrated the causes of Aβ accumulation in early onset familial AD (FAD) patients as autosomal dominant gene mutations lead to increased Aβ42 production (52, 53). However, the majority of AD cases are sporadic and late-onset, and the pathological mechanisms that lead to Aβ accumulation are less clear. HSPGs are glycoproteins composed of a core protein coupled to one or more heparan sulfate glycosaminoglycan chains (12). Five distinct classes of HSPGs have been identified, including membrane HSPGs (such as syndecans and glypicans) and the secreted extracellular matrix HSPGs (agrin, perlecan, type XVIII collagen) (54). HSPGs have been shown to interact with a variety of molecules because of their highly sulfated nature, thereby mediating biological activities including endocytosis and cell signaling (12, 55, 56). In this study, we have provided *in vivo* evidence that neuronal depletion of HS leads to reduced Aβ and amyloid deposition in APP/PS1 amyloid model mice. Deficiency of neuronal HS did not affect APP processing and Aβ production but did enhance Aβ clearance. These results suggest that the association of Aβ and HSPGs on the surface of neurons likely suppresses or represents an inefficient pathway for Aβ clearance (Fig. S7). Also, neuronal HSPGs might facilitate Aβ oligomerization and aggregation (Fig. S7). Interestingly, Aβ40 was shown to inhibit the heparanase-mediated degradation of HS (31, 57). Thus, the increases of Aβ and HS may result in a vicious cycle that further contributes to the persistence and stability of amyloid plaques in AD brains.

Aβ is mainly generated in neurons and eliminated from the brain through several clearance pathways (6, 46, 58-60); one of the major pathways depends on enzymatic degradation in ISF by proteases such as neprilysin and insulin degrading enzyme (61). Thus, the interactions of Aβ with other molecules are predicted to interfere with the enzymatic degradation machineries by physically blocking their association sites. In fact, HSPGs have been proposed to function as a chaperone that serves as a protective shield against the proteolytic degradation of Aβ; thus, the clearance of Aβ is likely hindered in the presence of cell surface HSPGs (47, 62) (Fig. S7). Consistent with this notion, our results demonstrated that deficiency of neuronal HS accelerates Aβ elimination in the mouse hippocampus. Intriguingly, we found that deletion of HS in neurons exacerbated CAA formation in spite of the reduction of Aβ and amyloid plaque deposition in the brain parenchyma. Given that significant portions of ISF Aβ flows along the cerebral vasculature and is cleared into the blood flow through the blood-brain barrier (BBB) or the perivascular drainage pathway (63, 64), Aβ likely is deposited on cerebrovasculature as CAA when these pathways are disturbed or the amount of drained Aβ overwhelms the clearance capacity. Our results suggest that the expression of HSPGs in various brain compartments might play an important role in regulating the distribution of Aβ in the brain. HSPGs on the surface of the neurons likely capture Aβ and serve as a reservoir for Aβ accumulation in brain parenchyma. When this pathway is absent, the drainage of ISF Aβ into the perivascular

regions is likely enhanced. Specific HSPGs have been shown to be prominent within the cerebral microvasculature and are involved in BBB maintenance, permeability and the pathogenesis of CAA (31, 49). It is possible that the remaining HSPGs in the microvascular network of the brain contribute to the deposition of cerebrovascular amyloid in the APP/PS1; n$Ext1^{CKO}$ mice. Our neuronal HS-deficient mouse model provides further insight into the dynamic distribution of Aβ, and the potential mechanisms by which HSPGs in different brain compartments might mediate Aβ metabolism *in vivo*. Whether vascular HSPGs directly affect BBB integrity, the perivascular drainage clearance of Aβ and CAA formation *in vivo* warrants further investigation.

HSPGs have also been suggested to function as a catalyst to promote Aβ oligomer formation and aggregation (23, 62, 65). *In vitro* experiments have shown that HS accelerates Aβ aggregation through their direct interaction (20-22). Membrane bound glypican-1 has been shown to interact with oligomerized Aβ in the detergent-insoluble glycosphingolipid-enriched compartment (20). Agrin, an extracellular matrix HSPG, has been found to bind to Aβ and accelerated its fibril formation in human AD brain (16). Indeed, several HSPGs co-localize with senile plaques in AD brains (36, 66). Importantly, we also demonstrated that several subtypes of HSPGs, including syndecan-3, syndecan-4, glypican-1 and glypican-3, were significantly higher in AD human brain tissues, particularly in the pools of detergent-insoluble fractions compared to those in control individuals. These results suggest that aberrant amounts of HSPGs and their altered distribution in AD brains might contribute to Aβ aggregation and plaque formation, although further studies are needed. It is also possible that amyloid plaques capture HSPGs or promote the accumulation of HSPG-expressing glial cells, resulting in an increase of HSPGs in AD brains (32).

Receptor-mediated cellular uptake and subsequent lysosomal degradation is another critical pathway for Aβ clearance (64). Whereas microglia and astrocytes actively internalize and clear Aβ, neurons also play a role in cellular Aβ clearance. As HSPG is one of the major players that capture Aβ on the cell surface of neurons for endocytosis (64, 67), the deficiency of HS in neurons seem to be disadvantageous for this clearance pathway. However, when excess amounts of Aβ are internalized, it can aggregate in lysosomes likely providing “seeds” to initiate further Aβ aggregation (68, 69). In addition, Aβ has been shown to be self-propagating and is transmitted from one neuron to another after its cellular uptake (70-72). Thus, although the neuronal uptake of Aβ through HSPGs can lead to trafficking to the lysosomes (25), albeit less efficiently than via the low-density lipoprotein receptor-related protein 1 (LRP1) (67), such a pathway might be harmful when the capacity for lysosomal degradation of Aβ is overwhelmed and compromised (Fig. 7S). It will be critical to investigate whether neuronal HSPGs mediate the propagation of Aβ during AD pathogenesis in future studies. Intriguingly, extracellular tau and α-synuclein have been shown to propagate after being endocytosed via cell surface HSPGs on neurons (56), which is likely to be a critical step for the progression of related neurodegenerative diseases (73). Thus, blocking the association of these pathogenic molecules with neuronal HSPGs may ameliorate the progression of various neurodegenerative diseases by preventing their propagation between neurons during disease development.

HSPGs interact with myriad molecules that orchestrate important biological functions (13). One limitation of our study is that we cannot rule out the possibility that disruption of HS binding to other molecules, in addition to Aβ, may also contribute to the modulation of Aβ metabolism in the adult mouse brain. One such molecule is apolipoprotein E (apoE) whose binding to HSPGs is known to contribute to the metabolism of apoE itself (64, 74). The ε4 allele of the *APOE* gene is the strongest genetic risk factor for sporadic AD among the three polymorphic alleles (ε2, ε3 and ε4). ApoE is required for seeding amyloid and has been shown to regulate Aβ metabolism and amyloid deposition in an apoE isoform-dependent manner (6, 75). Whether apoE is involved in HSPG-regulated Aβ metabolism/aggregation and whether this effect depends on apoE isoforms require further investigation.

In summary, our studies using genetically altered mice have clearly demonstrated a critical role of neuronal HS in brain Aβ clearance and oligomerization. Given that neuronal HSPGs are also likely involved in the pathogenic propagation of various proteins in neurodegenerative diseases and HSPGs are elevated in human brain tissues from AD patients, our studies establish a rationale for targeting the Aβ-HSPG pathway for therapy. Toward this end, it is interesting to note that the administration of a low-molecular-weight heparin reduced amyloid pathology in a mouse model of AD, likely by antagonizing Aβ-HSPG interactions (65). Given that HSPGs interact with myriad critical molecules that mediate diverse biological activities (55), it will be critical to design and identify compounds that specifically inhibit the interaction between Aβ and HSPGs for the treatment of neurodegenerative diseases. When combined with other strategies targeting Aβ, including immunotherapy, these approaches might allow for a reduction, if not elimination, of Aβ-related toxicity.

MATERIALS AND METHODS

Study design

This study aimed to investigate the role of HSPG in regulating brain Aβ metabolism using a conditional knockout mouse model. To accomplish this aim, the *Ext1* gene, which encodes an essential glycosyltransferase for HS biosynthesis, was genetically ablated in the forebrain neurons of APP/PS1 mice. The effects of neuronal HS deficiency on the amounts of Aβ, amyloid deposition and neuroinflammation were assessed by Aβ ELISAs, immunohistochemistry, real-time PCR, and Western blot analyses. The neuronal HS-deficient APP/PS1 mice exhibited dramatic reduction in amyloid oligomerization and deposition. Using *in vivo* microdialysis, we also detected an accelerated rate of Aβ clearance in the brain ISF of HS-deficient mice, suggesting that neuronal HS might represent an inefficient or inhibitory pathway for Aβ clearance. We further examined the amounts of various HSPG species in postmortem human brain tissues from control and AD patients using specific ELISAs to evaluate the potential relevance of altered HSPGs in AD pathogenesis. The mice of different genotypes were selected on the basis of availability. Sample sizes were adequately powered to observe the effects on the basis of past experience of animal studies (67, 76). Data collection and the quantification of immunoreactivity for mouse samples were performed with the investigators unaware of the sample identities until statistical analyses.

Human postmortem brain tissues

Temporal lobe cortical samples from neurologically unimpaired subjects (n = 20) and from subjects with AD (n = 20) were obtained from the University of Kentucky Alzheimer's Disease Center (ADC) Neuropathology Core (Lexington, Kentucky, USA) (76). After autopsy, the samples were snap frozen in liquid nitrogen and kept frozen at -80°C. Informed consent was obtained through ADC Neuropathology Core, and we obtained institutional review board approval to use these brain samples for research. Diagnosis of AD was confirmed by pathological and clinical criteria as described (77). The average age of subjects was 85.1 ± 5.7 years in the control group and 84.4 ± 5.2 years in the AD group (p = 0.69). Average postmortem interval was 3.2 hr and was not significantly different between the two groups (p = 0.22).

Animals

All animal procedures were approved by the Mayo Clinic Institutional Animal Care and Use Committee (IACUC) and were in accordance with the National Institutes of Health Guide for the Care and Use of Laboratory Animals. *Ext1*$^{flox/flox}$ mice have been described in previous studies (27). Double transgenic APPswe/PS1ΔE9 (APP/PS1) mice were purchased from The Jackson Laboratory and were initially generated by Jankowsky et al. as described (29).

In vivo Aβ microdialysis

To assess ISF Aβ in the hippocampus of awake, freely moving APP/PS1 and APP/PS1; n*Ext1*^{CKO} mice, *in vivo* microdialysis was performed as previously described (8, 44). Briefly, under isoflurane volatile anesthetic, guide cannula (BR style; Bioanalytical Systems) were cemented into the hippocampus (3.1 mm behind bregma, 2.5 mm lateral to midline, and 1.2 mm below dura at a 12° angle). A microdialysis probe (38-kDa molecular weight cut-off membrane; Bioanalytical Systems) was inserted through the guide cannula into the brain. Artificial CSF (mM: 1.3 $CaCl_2$, 1.2 $MgSO_4$, 3 KCl, 0.4 KH_2PO_4, 25 $NaHCO_3$, and 122 NaCl, pH 7.35) containing 4% BSA (Sigma) filtered through a 0.1 μm membrane was used as microdialysis perfusion buffer. Flow rate was a constant 1.0 μL/min. Samples were collected every 60-90 min overnight which gets through the 4-6 hr recovery period and the mean concentration of Aβ over the 6 hr preceding treatment was defined as basal concentration of ISF Aβ. Sample were collected through a refrigerated fraction collector and assessed for Aβ40 or Aβ42 by ELISAs. For each animal, all Aβ concentration was normalized to the basal Aβ concentration. To measure Aβ elimination half-life, mice were administered a γ-secretase inhibitor, LY411575 (5 mg/kg) intraperitoneally to rapidly block the production of Aβ. Microdialysis samples were collected every 60 min for 6 hr. The half-life of ISF Aβ was calculated on the basis of the slope of the semi-log plot of % change in Aβ versus time (8).

ELISA quantification

ISF Aβ concentration was assessed using sandwich Aβ40 or Aβ42 specific ELISAs as described (44). Briefly, a mouse anti-Aβ40 antibody HJ2 (anti-Aβ35-40) or Aβ42 antibody HJ7.4 (anti-Aβ37-42) was used as capture antibody, respectively. A biotinylated antibody

HJ5.1 (anti-Aβ13-28) targeting the central domain of Aβ was used as the detecting antibody, followed by ELISA development using streptavidin-poly-HRP-40 (Fitzgerald Industries). Synthetic human Aβ40 or Aβ42 peptide (American Peptide) was used to generate the standard curves for each assay. The ELISA assays were developed using Super Slow ELISA TMB (Sigma) with absorbance read on a Bio-Tek plate reader. The Aβ concentration in the brain lysates was determined by ELISA (78) with end-specific mAb 2.1.3 (human Aβx-42 specific) and mAb 13.1.1 (human Aβx-40 specific) for capture and HRP-conjugated mAb Ab5 (human Aβ1-16 specific) for detection. The ELISAs were developed using Super Slow ELISA TMB (Sigma). To detect soluble oligomeric Aβ species, the same antibody, 3D6 (to Aβ residues 1-5), was used for both capture and detection similarly to previously described (40). Briefly, 3D6 (10 μg/ml) antibody was coated into 96-well immunoassay plates overnight at 4°C. The plates were then aspirated and blocked with 4% BSA in PBS buffer for at least 1 hr at 37°C. The samples and standards were added to the plates and incubated overnight at 4°C. The Aβ oligomers used as standards were prepared and characterized as previously described (79, 80). The plates were washed three or more times with wash buffer between each step of the assay. The plate was incubated with the biotinylated 3D6 (0.5 μg/ml) antibody in assay buffer (0.25% casein/0.05% Tween 20, pH 7.4, in PBS) for 90 min at 37°C. The avidin-horseradish peroxidase (Vector Laboratories) was added to the wells for 90 min at RT. The ELISAs were developed using Super Slow ELISA TMB (Sigma). To measure total Aβ amount, 3D6 (10 μg/ml) and biotinylated mAb 266 (to Aβ residues 13-28, 0.5 μg/ml) were used as the capture and detection antibodies, respectively. All procedures were the same as those in oligomeric Aβ ELISA described above.

Preparation of brain homogenates

Mouse brain tissues and human postmortem brain tissues were processed through sequential extraction as described (38). Frozen brain tissues were homogenized with TBS, and centrifuged at 100,000 x g for 60 min at 4°C with supernatant defined as TBS-soluble fraction. Pellets were re-suspended in TBS buffer containing 1% Triton X-100 (TBSX) and mixed gently by rotation at 4°C for 30 min, followed by a second centrifugation at 100,000 x g for 60 min with supernatant defined as TBSX-soluble fraction. The TBSX-insoluble pellet was re-suspended with 5 M guanidine, mixed by rotation at room temperature overnight, and centrifuged at 16,000 x g for 30 min with supernatant defined as GDN-soluble fraction.

Immunohistochemical and immunofluorescence staining and analyses

Paraffin embedded sections were immunostained using pan-Aβ (Aβ 33.1.1; human Aβ 1-16 specific), anti-GFAP (BioGenex), anti-Aβ40 (Millipore), anti-Aβ42 (21F12, kindly provided by Eli Lilly) and anti-ionized calcium-binding adaptor molecule 1 (Iba-1) (Wako) antibodies (81). Immunohistochemically stained sections were captured using the ImageScope AT2 image scanner (Aperio Technologies) and analyzed using the ImageScope software. The intensities of GFAP and Iba-1 staining in the hippocampus were calculated using the Positive Pixel Count program available with the ImageScope software (Aperio Technologies) (81). The fibrillar Aβ was immunostained with Thioflavin S. The images were captured by Aperio Fluorescent Scanner and the stained areas covered by the fibrillary plaque were quantified by Image J. For examining the CAA in the cerebral vasculature, paraffin embedded sections were co-stained with α-SMA antibody (Abcam) and Aβ

antibody (MOAB2), followed by Alexa Fluor 488- and 568-conjugated secondary antibodies (Invitrogen). MOAB2 antibody was a kind gift from Dr. Mary Jo LaDu (University of Illinois at Chicago). The images were acquired by a confocal laser-scanning fluorescence microscope (model LSM510 invert; Carl Zeiss, Germany).

Statistical analysis

All quantified data represent an average of samples. Statistical analyses were performed with Excel or GraphPad Prism software. Statistical significance was determined by two-tailed Student's t test. Levels of significance: $*P < 0.05$; $**P < 0.01$; $P < 0.05$ was considered significant.

Supplementary Material

Refer to Web version on PubMed Central for supplementary material.

Acknowledgments

This work was supported by NIH grants P01NS074969, R01AG027924, R01AG035355, R01AG046205, P50AG016574, and grants from the Alzheimer's Association and Cure Alzheimer's Fund (to G.B.), NIH grant R01NS088496 (to Y. Y.), NIH grant R01AG042513 (to J.R.C.), Mayo Clinic CRM Career Development Award (to T.K.), and a fellowship from the American Heart Association (to C.-C.L.). We thank Steven Estus (University of Kentucky) and University of Kentucky Alzheimers Disease Center (P30 AG028383) for providing postmortem human brain tissues, Mary Jo LaDu (University of Illinois at Chicago) for providing MOAB2 antibody, and Pritam Das for providing γ-secretase inhibitor, LY411575. We are grateful to Dennis Dickson, Monica Castanedes Casey, Linda Rousseau, and Virginia Phillips for histology and immunohistochemical analyses. We also thank Mary Davis for careful reading of this manuscript.

REFERENCES AND NOTES

1. Hardy J, Selkoe DJ. The amyloid hypothesis of Alzheimer's disease: progress and problems on the road to therapeutics. Science. 2002; 297:353–356. [PubMed: 12130773]
2. Selkoe DJ. Deciphering the genesis and fate of amyloid beta-protein yields novel therapies for Alzheimer disease. J Clin Invest. 2002; 110:1375–1381. [PubMed: 12438432]
3. Vassar R, Bennett BD, Babu-Khan S, Kahn S, Mendiaz EA, Denis P, Teplow DB, Ross S, Amarante P, Loeloff R, Luo Y, Fisher S, Fuller J, Edenson S, Lile J, Jarosinski MA, Biere AL, Curran E, Burgess T, Louis JC, Collins F, Treanor J, Rogers G, Citron M. Beta-secretase cleavage of Alzheimer's amyloid precursor protein by the transmembrane aspartic protease BACE. Science. 1999; 286:735–741. [PubMed: 10531052]
4. Kimberly WT, LaVoie MJ, Ostaszewski BL, Ye W, Wolfe MS, Selkoe DJ. Gamma-secretase is a membrane protein complex comprised of presenilin, nicastrin, Aph-1, and Pen-2. Proc Natl Acad Sci U S A. 2003; 100:6382–6387. [PubMed: 12740439]
5. Goate A. Segregation of a missense mutation in the amyloid beta-protein precursor gene with familial Alzheimer's disease. J Alzheimers Dis. 2006; 9:341–347. [PubMed: 16914872]
6. Bu G. Apolipoprotein E and its receptors in Alzheimer's disease: pathways, pathogenesis and therapy. Nat Rev Neurosci. 2009; 10:333–344. [PubMed: 19339974]
7. Mucke L, Selkoe DJ. Neurotoxicity of amyloid beta-protein: synaptic and network dysfunction. Cold Spring Harb Perspect Med. 2012; 2:a006338. [PubMed: 22762015]
8. Cirrito JR, May PC, O'Dell MA, Taylor JW, Parsadanian M, Cramer JW, Audia JE, Nissen JS, Bales KR, Paul SM, DeMattos RB, Holtzman DM. In vivo assessment of brain interstitial fluid with microdialysis reveals plaque-associated changes in amyloid-beta metabolism and half-life. J Neurosci. 2003; 23:8844–8853. [PubMed: 14523085]

9. Bateman RJ, Munsell LY, Morris JC, Swarm R, Yarasheski KE, Holtzman DM. Human amyloid-beta synthesis and clearance rates as measured in cerebrospinal fluid in vivo. Nat Med. 2006; 12:856–861. [PubMed: 16799555]
10. Mawuenyega KG, Sigurdson W, Ovod V, Munsell L, Kasten T, Morris JC, Yarasheski KE, Bateman RJ. Decreased clearance of CNS beta-amyloid in Alzheimer's disease. Science. 2010; 330:1774. [PubMed: 21148344]
11. Park PW, Reizes O, Bernfield M. Cell surface heparan sulfate proteoglycans: selective regulators of ligand-receptor encounters. J Biol Chem. 2000; 275:29923–29926. [PubMed: 10931855]
12. Sarrazin S, Lamanna WC, Esko JD. Heparan sulfate proteoglycans. Cold Spring Harb Perspect Biol. 2011; 3
13. Bishop JR, Schuksz M, Esko JD. Heparan sulphate proteoglycans fine-tune mammalian physiology. Nature. 2007; 446:1030–1037. [PubMed: 17460664]
14. Lind T, Tufaro F, McCormick C, Lindahl U, Lidholt K. The putative tumor suppressors EXT1 and EXT2 are glycosyltransferases required for the biosynthesis of heparan sulfate. J Biol Chem. 1998; 273:26265–26268. [PubMed: 9756849]
15. Lin X, Wei G, Shi Z, Dryer L, Esko JD, Wells DE, Matzuk MM. Disruption of gastrulation and heparan sulfate biosynthesis in EXT1-deficient mice. Dev Biol. 2000; 224:299–311. [PubMed: 10926768]
16. Cotman SL, Halfter W, Cole GJ. Agrin binds to beta-amyloid (Abeta), accelerates abeta fibril formation, and is localized to Abeta deposits in Alzheimer's disease brain. Mol Cell Neurosci. 2000; 15:183–198. [PubMed: 10673326]
17. van Horssen J, Otte-Holler I, David G, Maat-Schieman ML, van den Heuvel LP, Wesseling P, de Waal RM, Verbeek MM. Heparan sulfate proteoglycan expression in cerebrovascular amyloid beta deposits in Alzheimer's disease and hereditary cerebral hemorrhage with amyloidosis (Dutch) brains. Acta Neuropathol. 2001; 102:604–614. [PubMed: 11761721]
18. Van Gool D, David G, Lammens M, Baro F, Dom R. Heparan sulfate expression patterns in the amyloid deposits of patients with Alzheimer's and Lewy body type dementia. Dementia. 1993; 4:308–314. [PubMed: 8136893]
19. Zhang GL, Zhang X, Wang XM, Li JP. Towards understanding the roles of heparan sulfate proteoglycans in Alzheimer's disease. Biomed Res Int. 2014; 2014 516028.
20. Watanabe N, Araki W, Chui DH, Makifuchi T, Ihara Y, Tabira T. Glypican-1 as an Abeta binding HSPG in the human brain: its localization in DIG domains and possible roles in the pathogenesis of Alzheimer's disease. Faseb J. 2004; 18:1013–1015. [PubMed: 15084524]
21. Cheng F, Ruscher K, Fransson LA, Mani K. Non-toxic amyloid beta formed in the presence of glypican-1 or its deaminatively generated heparan sulfate degradation products. Glycobiology. 2013; 23:1510–1519. [PubMed: 24026238]
22. Brunden KR, Richter-Cook NJ, Chaturvedi N, Frederickson RC. pH-dependent binding of synthetic beta-amyloid peptides to glycosaminoglycans. J Neurochem. 1993; 61:2147–2154. [PubMed: 8245966]
23. Sandwall E, O'Callaghan P, Zhang X, Lindahl U, Lannfelt L, Li JP. Heparan sulfate mediates amyloid-beta internalization and cytotoxicity. Glycobiology. 2010; 20:533–541. [PubMed: 20053627]
24. Bergamaschini L, Donarini C, Rossi E, De Luigi A, Vergani C, De Simoni MG. Heparin attenuates cytotoxic and inflammatory activity of Alzheimer amyloid-beta in vitro. Neurobiol Aging. 2002; 23:531–536. [PubMed: 12009502]
25. Kanekiyo T, Zhang J, Liu Q, Liu CC, Zhang L, Bu G. Heparan sulphate proteoglycan and the low-density lipoprotein receptor-related protein 1 constitute major pathways for neuronal amyloid-beta uptake. J Neurosci. 2011; 31:1644–1651. [PubMed: 21289173]
26. Jendresen CB, Cui H, Zhang X, Vlodavsky I, Nilsson LN, Li JP. Overexpression of heparanase lowers the amyloid burden in amyloid-beta precursor protein transgenic mice. J Biol Chem. 2015; 290:5053–5064. [PubMed: 25548284]
27. Inatani M, Irie F, Plump AS, Tessier-Lavigne M, Yamaguchi Y. Mammalian brain morphogenesis and midline axon guidance require heparan sulfate. Science. 2003; 302:1044–1046. [PubMed: 14605369]

28. Tsien JZ, Chen DF, Gerber D, Tom C, Mercer EH, Anderson DJ, Mayford M, Kandel ER, Tonegawa S. Subregion- and cell type-restricted gene knockout in mouse brain. Cell. 1996; 87:1317–1326. [PubMed: 8980237]
29. Jankowsky JL, Fadale DJ, Anderson J, Xu GM, Gonzales V, Jenkins NA, Copeland NG, Lee MK, Younkin LH, Wagner SL, Younkin SG, Borchelt DR. Mutant presenilins specifically elevate the levels of the 42 residue beta-amyloid peptide in vivo: evidence for augmentation of a 42-specific gamma secretase. Hum Mol Genet. 2004; 13:159–170. [PubMed: 14645205]
30. Irie F, Badie-Mahdavi H, Yamaguchi Y. Autism-like socio-communicative deficits and stereotypies in mice lacking heparan sulfate. Proc Natl Acad Sci U S A. 2012; 109:5052–5056. [PubMed: 22411800]
31. van Horssen J, Wesseling P, van den Heuvel LP, de Waal RM, Verbeek MM. Heparan sulphate proteoglycans in Alzheimer's disease and amyloid-related disorders. Lancet Neurol. 2003; 2:482–492. [PubMed: 12878436]
32. O'Callaghan P, Sandwall E, Li JP, Yu H, Ravid R, Guan ZZ, van Kuppevelt TH, Nilsson LN, Ingelsson M, Hyman BT, Kalimo H, Lindahl U, Lannfelt L, Zhang X. Heparan sulfate accumulation with Abeta deposits in Alzheimer's disease and Tg2576 mice is contributed by glial cells. Brain Pathol. 2008; 18:548–561. [PubMed: 18422760]
33. Garcia-Alloza M, Robbins EM, Zhang-Nunes SX, Purcell SM, Betensky RA, Raju S, Prada C, Greenberg SM, Bacskai BJ, Frosch MP. Characterization of amyloid deposition in the APPswe/PS1dE9 mouse model of Alzheimer disease. Neurobiol Dis. 2006; 24:516–524. [PubMed: 17029828]
34. Youmans KL, Tai LM, Kanekiyo T, Stine WB Jr, Michon SC, Nwabuisi-Heath E, Manelli AM, Fu Y, Riordan S, Eimer WA, Binder L, Bu G, Yu C, Hartley DM, LaDu MJ. Intraneuronal Abeta detection in 5xFAD mice by a new Abeta-specific antibody. Mol Neurodegener. 2012; 7:8. [PubMed: 22423893]
35. Timmer NM, Herbert MK, Kleinovink JW, Kiliaan AJ, De Waal RM, Verbeek MM. Limited expression of heparan sulphate proteoglycans associated with Abeta deposits in the APPswe/PS1dE9 mouse model for Alzheimer's disease. Neuropathol Appl Neurobiol. 2010; 36:478–486. [PubMed: 20831743]
36. Verbeek MM, Otte-Holler I, van den Born J, van den Heuvel LP, David G, Wesseling P, de Waal RM. Agrin is a major heparan sulfate proteoglycan accumulating in Alzheimer's disease brain. Am J Pathol. 1999; 155:2115–2125. [PubMed: 10595940]
37. Rauch SM, Huen K, Miller MC, Chaudry H, Lau M, Sanes JR, Johanson CE, Stopa EG, Burgess RW. Changes in brain beta-amyloid deposition and aquaporin 4 levels in response to altered agrin expression in mice. J Neuropathol Exp Neurol. 2011; 70:1124–1137. [PubMed: 22082664]
38. Youmans KL, Leung S, Zhang J, Maus E, Baysac K, Bu G, Vassar R, Yu C, LaDu MJ. Amyloid-beta42 alters apolipoprotein E solubility in brains of mice with five familial AD mutations. J Neurosci Methods. 2011; 196:51–59. [PubMed: 21219931]
39. Selkoe DJ. Soluble oligomers of the amyloid beta-protein impair synaptic plasticity and behavior. Behav Brain Res. 2008; 192:106–113. [PubMed: 18359102]
40. Xia W, Yang T, Shankar G, Smith IM, Shen Y, Walsh DM, Selkoe DJ. A specific enzyme-linked immunosorbent assay for measuring beta-amyloid protein oligomers in human plasma and brain tissue of patients with Alzheimer disease. Arch Neurol. 2009; 66:190–199. [PubMed: 19204155]
41. Castillo GM, Lukito W, Wight TN, Snow AD. The sulfate moieties of glycosaminoglycans are critical for the enhancement of beta-amyloid protein fibril formation. J Neurochem. 1999; 72:1681–1687. [PubMed: 10098877]
42. Wyss-Coray T. Inflammation in Alzheimer disease: driving force, bystander or beneficial response? Nat Med. 2006; 12:1005–1015. [PubMed: 16960575]
43. Rubio-Perez JM, Morillas-Ruiz JM. A review: inflammatory process in Alzheimer's disease, role of cytokines. ScientificWorldJournal. 2012; 2012 756357.
44. Cirrito JR, Disabato BM, Restivo JL, Verges DK, Goebel WD, Sathyan A, Hayreh D, D'Angelo G, Benzinger T, Yoon H, Kim J, Morris JC, Mintun MA, Sheline YI. Serotonin signaling is associated with lower amyloid-beta levels and plaques in transgenic mice and humans. Proc Natl Acad Sci U S A. 2011; 108:14968–14973. [PubMed: 21873225]

45. Bero AW, Yan P, Roh JH, Cirrito JR, Stewart FR, Raichle ME, Lee JM, Holtzman DM. Neuronal activity regulates the regional vulnerability to amyloid-beta deposition. Nat Neurosci. 2011; 14:750–756. [PubMed: 21532579]
46. Weller RO, Subash M, Preston SD, Mazanti I, Carare RO. Perivascular drainage of amyloid-beta peptides from the brain and its failure in cerebral amyloid angiopathy and Alzheimer's disease. Brain Pathol. 2008; 18:253–266. [PubMed: 18363936]
47. Snow AD, Sekiguchi RT, Nochlin D, Kalaria RN, Kimata K. Heparan sulfate proteoglycan in diffuse plaques of hippocampus but not of cerebellum in Alzheimer's disease brain. Am J Pathol. 1994; 144:337–347. [PubMed: 8311117]
48. Snow AD, Mar H, Nochlin D, Kimata K, Kato M, Suzuki S, Hassell J, Wight TN. The presence of heparan sulfate proteoglycans in the neuritic plaques and congophilic angiopathy in Alzheimer's disease. Am J Pathol. 1988; 133:456–463. [PubMed: 2974240]
49. Donahue JE, Berzin TM, Rafii MS, Glass DJ, Yancopoulos GD, Fallon JR, Stopa EG. Agrin in Alzheimer's disease: altered solubility and abnormal distribution within microvasculature and brain parenchyma. Proc Natl Acad Sci U S A. 1999; 96:6468–6472. [PubMed: 10339611]
50. Huang Y, Mucke L. Alzheimer mechanisms and therapeutic strategies. Cell. 2012; 148:1204–1222. [PubMed: 22424230]
51. Holtzman DM, Morris JC, Goate AM. Alzheimer's disease: the challenge of the second century. Sci Transl Med. 2011; 3:77sr71.
52. Citron M, Oltersdorf T, Haass C, McConlogue L, Hung AY, Seubert P, Vigo-Pelfrey C, Lieberburg I, Selkoe DJ. Mutation of the beta-amyloid precursor protein in familial Alzheimer's disease increases beta-protein production. Nature. 1992; 360:672–674. [PubMed: 1465129]
53. Campion D, Dumanchin C, Hannequin D, Dubois B, Belliard S, Puel M, Thomas-Anterion C, Michon A, Martin C, Charbonnier F, Raux G, Camuzat A, Penet C, Mesnage V, Martinez M, Clerget-Darpoux F, Brice A, Frebourg T. Early-onset autosomal dominant Alzheimer disease: prevalence, genetic heterogeneity, and mutation spectrum. Am J Hum Genet. 1999; 65:664–670. [PubMed: 10441572]
54. Iozzo RV. Heparan sulfate proteoglycans: intricate molecules with intriguing functions. J Clin Invest. 2001; 108:165–167. [PubMed: 11457866]
55. Turnbull J, Powell A, Guimond S. Heparan sulfate: decoding a dynamic multifunctional cell regulator. Trends Cell Biol. 2001; 11:75–82. [PubMed: 11166215]
56. Holmes BB, DeVos SL, Kfoury N, Li M, Jacks R, Yanamandra K, Ouidja MO, Brodsky FM, Marasa J, Bagchi DP, Kotzbauer PT, Miller TM, Papy-Garcia D, Diamond MI. Heparan sulfate proteoglycans mediate internalization and propagation of specific proteopathic seeds. Proc Natl Acad Sci U S A. 2013; 110:E3138–3147. [PubMed: 23898162]
57. Bame KJ, Danda J, Hassall A, Tumova S. Abeta(1-40) prevents heparanase-catalyzed degradation of heparan sulfate glycosaminoglycans and proteoglycans in vitro. A role for heparan sulfate proteoglycan turnover in Alzheimer's disease. J Biol Chem. 1997; 272:17005–17011. [PubMed: 9202014]
58. Cirrito JR, Deane R, Fagan AM, Spinner ML, Parsadanian M, Finn MB, Jiang H, Prior JL, Sagare A, Bales KR, Paul SM, Zlokovic BV, Piwnica-Worms D, Holtzman DM. P-glycoprotein deficiency at the blood-brain barrier increases amyloid-beta deposition in an Alzheimer disease mouse model. J Clin Invest. 2005; 115:3285–3290. [PubMed: 16239972]
59. Farris W, Schutz SG, Cirrito JR, Shankar GM, Sun X, George A, Leissring MA, Walsh DM, Qiu WQ, Holtzman DM, Selkoe DJ. Loss of neprilysin function promotes amyloid plaque formation and causes cerebral amyloid angiopathy. Am J Pathol. 2007; 171:241–251. [PubMed: 17591969]
60. Miners JS, Baig S, Palmer J, Palmer LE, Kehoe PG, Love S. Abeta-degrading enzymes in Alzheimer's disease. Brain Pathol. 2008; 18:240–252. [PubMed: 18363935]
61. Saido T, Leissring MA. Proteolytic degradation of amyloid beta-protein. Cold Spring Harb Perspect Med. 2012; 2:a006379. [PubMed: 22675659]
62. Gupta-Bansal R, Frederickson RC, Brunden KR. Proteoglycan-mediated inhibition of A beta proteolysis. A potential cause of senile plaque accumulation. J Biol Chem. 1995; 270:18666–18671. [PubMed: 7629198]

63. Sagare AP, Bell RD, Zlokovic BV. Neurovascular dysfunction and faulty amyloid beta-peptide clearance in Alzheimer disease. Cold Spring Harb Perspect Med. 2012; 2
64. Kanekiyo T, Xu H, Bu G. ApoE and Abeta in Alzheimer's disease: accidental encounters or partners? Neuron. 2014; 81:740–754. [PubMed: 24559670]
65. Bergamaschini L, Rossi E, Storini C, Pizzimenti S, Distaso M, Perego C, De Luigi A, Vergani C, De Simoni MG. Peripheral treatment with enoxaparin, a low molecular weight heparin, reduces plaques and beta-amyloid accumulation in a mouse model of Alzheimer's disease. J Neurosci. 2004; 24:4181–4186. [PubMed: 15115813]
66. van Horssen J, Wesseling P, van den Heuvel LP, de Waal RM, Verbeek MM. Heparan sulphate proteoglycans in Alzheimer's disease and amyloid-related disorders. Lancet Neurol. 2003; 2:482–492. [PubMed: 12878436]
67. Kanekiyo T, Cirrito JR, Liu CC, Shinohara M, Li J, Schuler DR, Holtzman DM, Bu G. Neuronal clearance of amyloid-beta by endocytic receptor LRP1. J Neurosci. 2013; 33:19276–19283. [PubMed: 24305823]
68. Hu X, Crick SL, Bu G, Frieden C, Pappu RV, Lee JM. Amyloid seeds formed by cellular uptake, concentration, and aggregation of the amyloid-beta peptide. Proc Natl Acad Sci U S A. 2009; 106:20324–20329. [PubMed: 19910533]
69. Li J, Kanekiyo T, Shinohara M, Zhang Y, LaDu MJ, Xu H, Bu G. Differential regulation of amyloid-beta endocytic trafficking and lysosomal degradation by apolipoprotein E isoforms. J Biol Chem. 2012; 287:44593–44601. [PubMed: 23132858]
70. Watts JC, Condello C, Stohr J, Oehler A, Lee J, DeArmond SJ, Lannfelt L, Ingelsson M, Giles K, Prusiner SB. Serial propagation of distinct strains of Abeta prions from Alzheimer's disease patients. Proc Natl Acad Sci U S A. 2014; 111:10323–10328. [PubMed: 24982139]
71. Meyer-Luehmann M, Coomaraswamy J, Bolmont T, Kaeser S, Schaefer C, Kilger E, Neuenschwander A, Abramowski D, Frey P, Jaton AL, Vigouret JM, Paganetti P, Walsh DM, Mathews PM, Ghiso J, Staufenbiel M, Walker LC, Jucker M. Exogenous induction of cerebral beta-amyloidogenesis is governed by agent and host. Science. 2006; 313:1781–1784. [PubMed: 16990547]
72. Song HL, Shim S, Kim DH, Won SH, Joo S, Kim S, Jeon NL, Yoon SY. beta-Amyloid is transmitted via neuronal connections along axonal membranes. Ann Neurol. 2014; 75:88–97. [PubMed: 24114864]
73. Guo JL, Covell DJ, Daniels JP, Iba M, Stieber A, Zhang B, Riddle DM, Kwong LK, Xu Y, Trojanowski JQ, Lee VM. Distinct alpha-synuclein strains differentially promote tau inclusions in neurons. Cell. 2013; 154:103–117. [PubMed: 23827677]
74. Futamura M, Dhanasekaran P, Handa T, Phillips MC, Lund-Katz S, Saito H. Two-step mechanism of binding of apolipoprotein E to heparin: implications for the kinetics of apolipoprotein E-heparan sulfate proteoglycan complex formation on cell surfaces. J Biol Chem. 2005; 280:5414–5422. [PubMed: 15583000]
75. Liu CC, Kanekiyo T, Xu H, Bu G. Apolipoprotein E and Alzheimer disease: risk, mechanisms and therapy. Nat Rev Neurol. 2013; 9:106–118. [PubMed: 23296339]
76. Liu CC, Tsai CW, Deak F, Rogers J, Penuliar M, Sung YM, Maher JN, Fu Y, Li X, Xu H, Estus S, Hoe HS, Fryer JD, Kanekiyo T, Bu G. Deficiency in LRP6-mediated Wnt signaling contributes to synaptic abnormalities and amyloid pathology in Alzheimer's disease. Neuron. 2014; 84:63–77. [PubMed: 25242217]
77. Grear KE, Ling IF, Simpson JF, Furman JL, Simmons CR, Peterson SL, Schmitt FA, Markesbery WR, Liu Q, Crook JE, Younkin SG, Bu G, Estus S. Expression of SORL1 and a novel SORL1 splice variant in normal and Alzheimers disease brain. Mol Neurodegener. 2009; 4:46. [PubMed: 19889229]
78. Das P, Verbeeck C, Minter L, Chakrabarty P, Felsenstein K, Kukar T, Maharvi G, Fauq A, Osborne BA, Golde TE. Transient pharmacologic lowering of Abeta production prior to deposition results in sustained reduction of amyloid plaque pathology. Mol Neurodegener. 2012; 7:39. [PubMed: 22892055]

79. Tay WM, Bryant JG, Martin PK, Nix AJ, Cusack BM, Rosenberry TL. A mass spectrometric approach for characterization of amyloid-beta aggregates and identification of their post-translational modifications. Biochemistry. 2012; 51:3759–3766. [PubMed: 22506642]

80. Rangachari V, Moore BD, Reed DK, Sonoda LK, Bridges AW, Conboy E, Hartigan D, Rosenberry TL. Amyloid-beta(1-42) rapidly forms protofibrils and oligomers by distinct pathways in low concentrations of sodium dodecylsulfate. Biochemistry. 2007; 46:12451–12462. [PubMed: 17910477]

81. Chakrabarty P, Ceballos-Diaz C, Beccard A, Janus C, Dickson D, Golde TE, Das P. IFN-gamma promotes complement expression and attenuates amyloid plaque deposition in amyloid beta precursor protein transgenic mice. J Immunol. 2010; 184:5333–5343. [PubMed: 20368278]

Accessible Summary

Neuronal HSPGs trap amyloid

The accumulation of neurotoxic amyloid-β (Aβ) in the brain is a pathological hallmark of Alzheimer's disease (AD). Heparan sulfate proteoglycans (HSPGs) are abundant cell surface receptors that co-localize with amyloid plaques. Here, Liu and colleagues show that genetically-engineered mice lacking heparan sulfates in forebrain neurons are protected from amyloid deposition because of a faster clearance of Aβ and reduction of Aβ aggregation. Also, the authors found that several HSPG species are increased in human AD brains. These findings suggest that targeting Aβ-HSPG interaction might be an effective strategy for AD prevention and treatment.

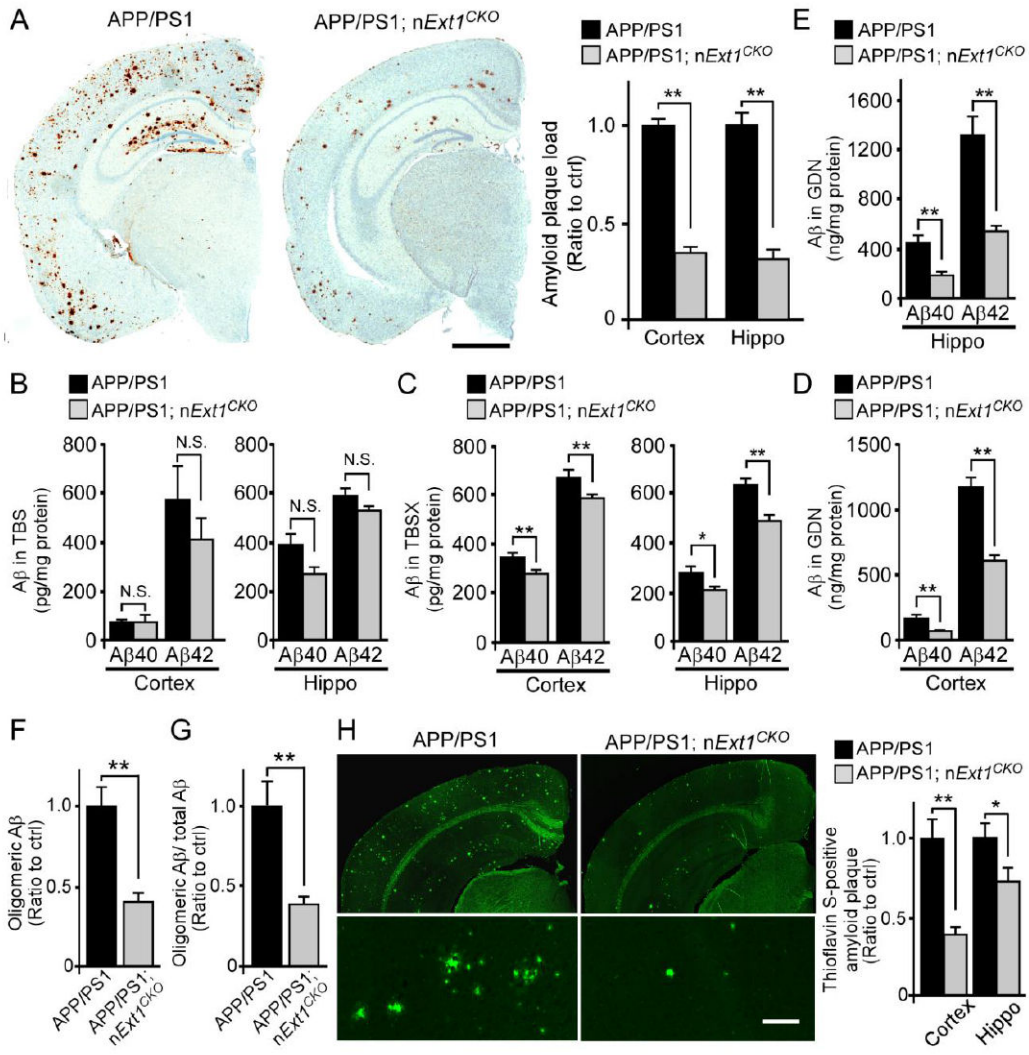

Fig. 1.

Neuronal HS deficiency reduces amyloid deposition. (**A**) Brain sections from control (APP/PS1) and neuronal HS-deficient (APP/PS1; n*Ext1*^{CKO}) mice (n=6-10/group) at 12 months of age were immunostained with a pan-Aβ antibody. Scale bar, 1 mm. The percentage of area covered by plaques was quantified, and the plaque load was normalized to that of APP/PS1 mice. (**B** to **E**) The cortical and hippocampal brain tissues of APP/PS1 and APP/PS1; n*Ext1*^{CKO} mice (n=7-12/group) at 12 months of age were fractionated into TBS-soluble, detergent-soluble (TBSX), and insoluble (guanidine-HCl, GDN) fractions. The amount of Aβ40 and Aβ42 in TBS (**B**), TBSX (**C**), and GDN (**D** to **E**) fractions was quantified by ELISA. (**F**) Soluble oligomeric Aβ in the cortex of APP/PS1 and APP/PS1; n*Ext1*^{CKO} mice (n=10-12/group). (**G**) The ratio of soluble oligomeric Aβ versus total Aβ in the TBS-soluble fraction in the cortex of APP/PS1 and APP/PS1; n*Ext1*^{CKO} mice (n=10-12/group). (**H**) Quantification of Thioflavin S-positive amyloid plaques in the cortex and hippocampus of APP/PS1 and APP/PS1; n*Ext1*^{CKO} mice (n=13/group) at 12 months of age. Scale bar, 100

μm. Values represent means ± SEM. N.S., not significant; *$P < 0.05$; **$P < 0.01$. Statistical analysis was performed using Student's t test.

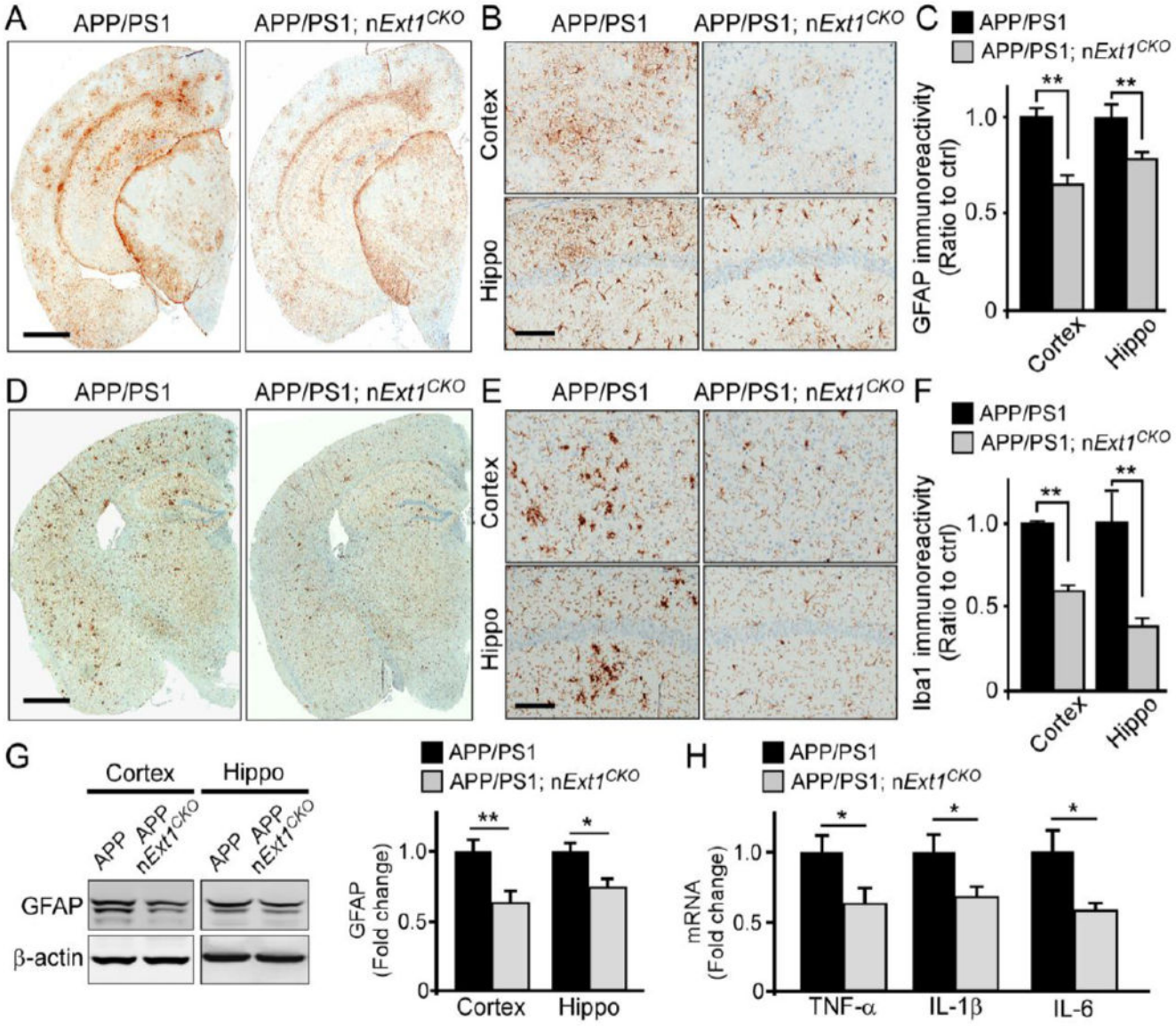

Fig. 2.

Deficiency of neuronal HS leads to reduced neuroinflammation. (**A** to **C**) Brain sections from APP/PS1 and APP/PS1; n*Ext1*^{CKO} mice at 12 months of age were immunostained with GFAP antibody. Scale bar, 1 mm. (**B**) Representative images of GFAP staining in the cortex and hippocampal CA1 region are shown. Scale bar, 1 mm. (**C**) Stained sections were scanned on the Aperio slide scanner and analyzed using the ImageScope software. The percentage of areas covered by GFAP staining in cortex (n=11-13/group) and hippocampus (n=7-10/group) were quantified. (**D** to **F**) Brain sections from APP/PS1 and APP/PS1; n*Ext1*^{CKO} mice at 12 months of age were immunostained with Iba1 antibody. Scale bar, 1 mm. (**E**) Representative images of Iba1 staining in the cortex and hippocampal CA1 region are shown. Scale bar, 100 m. (**F**) The percentage of area covered by Iba1 staining was quantified (n=4/group). (**G**) The amount of GFAP in the cortex (n= 9/group) and

hippocampus (n= 8-9/group) of APP/PS1 and APP/PS1; n*Ext1*^{CKO} mice examined by Western blot. (**H**) The amounts of TNF-α, IL-1β and IL-6 in the cortex of APP/PS1 and APP/PS1; n*Ext1*^{CKO} mice (n=6-8/group) evaluated by real-time PCR. Data represent mean ± SEM. **P* < 0.05; ***P* < 0.01. Statistical analysis was performed using Student's t test.

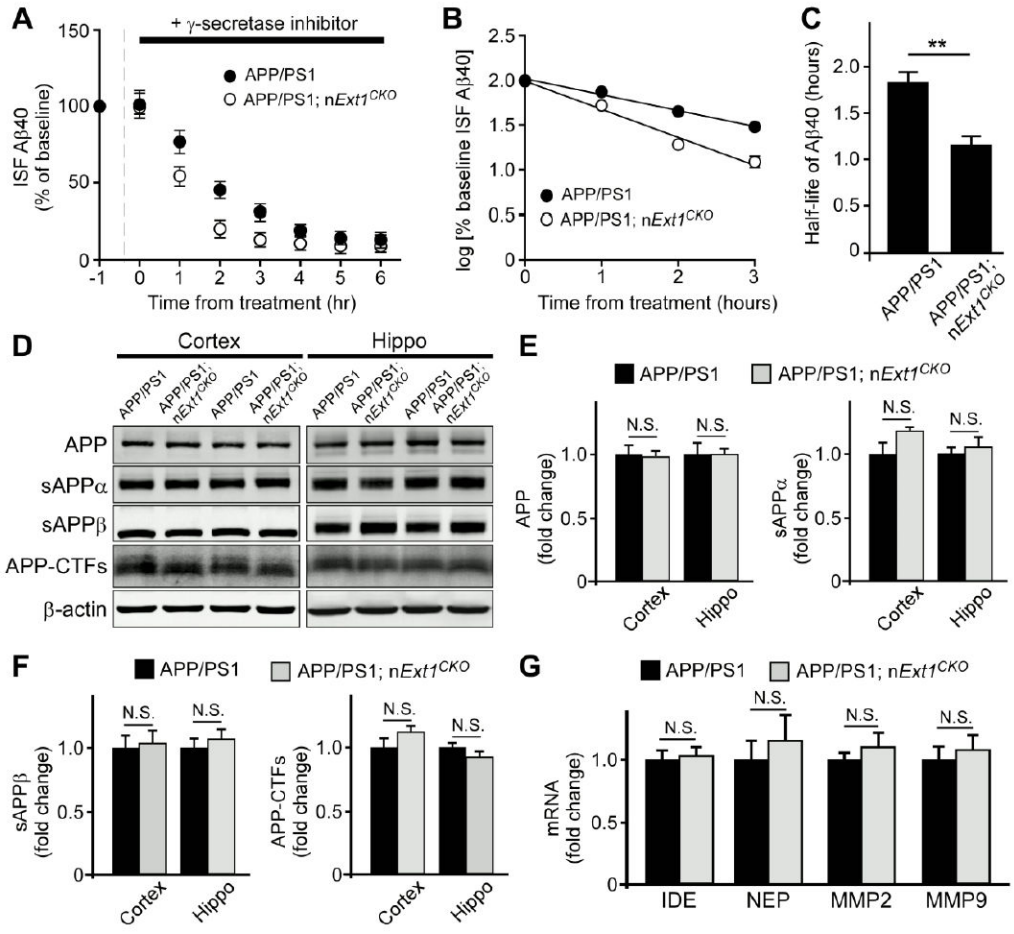

Fig. 3.

Deficiency of neuronal HS increases ISF Aβ clearance in the hippocampus of APP/PS1 mice. (**A** to **C**) APP/PS1 and APP/PS1; n*Ext1*^{CKO} mice (n= 8/group) were analyzed at the age of 3-4 months. To assess Aβ40 half-life, the mice were treated with a γ-secretase inhibitor, and the hippocampal ISF Aβ40 was monitored. ISF Aβ concentration during the hours of 9-16 after probe implantation were averaged and served as the basal amount of Aβ (shown as -1~0 hr) prior to γ-secretase injection (**A**). The common logarithm of percentage baseline ISF Aβ40 concentrations versus time was plotted (**B**). Data represent mean ± SEM. The slope from the individual linear regressions from log (% ISF Aβ40) versus time for each mouse was used to calculate the mean half-life ($t_{1/2}$) of elimination for Aβ from the ISF (**C**). Data represent mean ± SEM. $^{**}P < 0.01$. (**D** to **F**) Full-length APP, sAPPα, sAPPβ, CTF and β-actin were analyzed by Western blots in APP/PS1 and APP/PS1; n*Ext1*^{CKO} mice (n= 7-10/group) at 12 months of age. Densitometric quantification is expressed as mean ± SEM. (**G**) The mRNA of insulin degrading enzyme (IDE), neprilysin (NEP), MMP2 and MMP9 in the cortex of APP/PS1 and APP/PS1; n*Ext1*^{CKO} mice (n=8/group) evaluated by real-time PCR. N.S., not significant. Statistical analysis was performed using Student's t test.

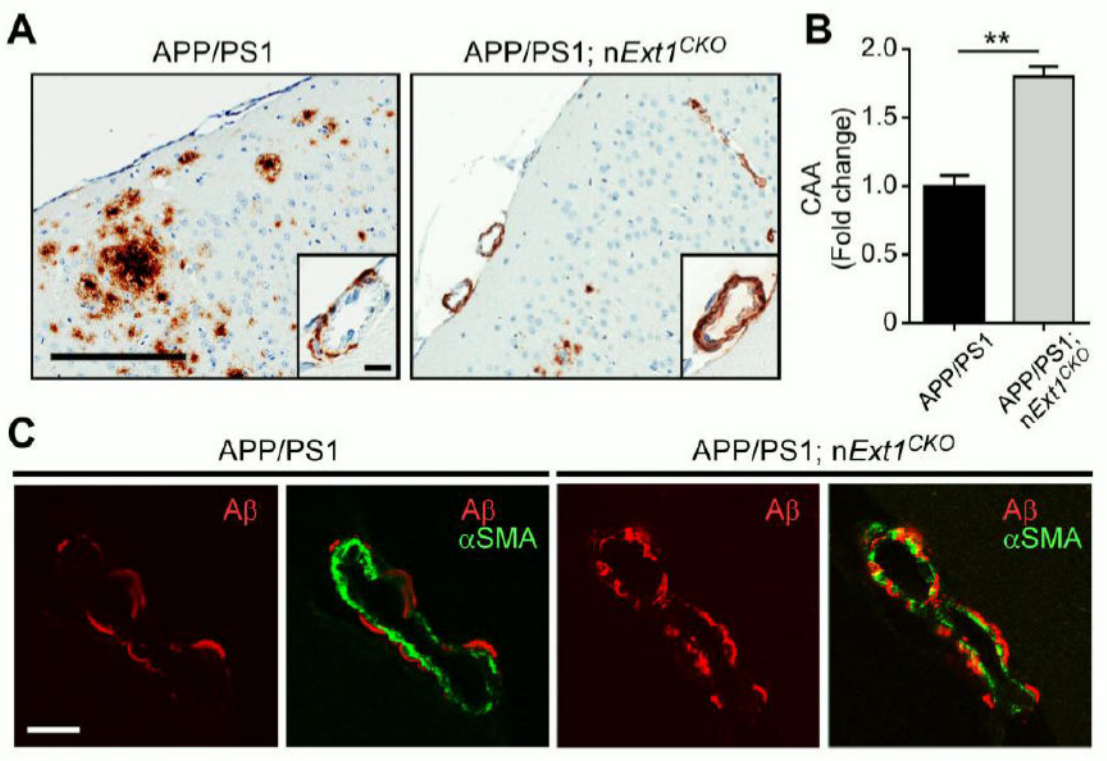

Fig. 4.

Deletion of neuronal HS increases the abundance of CAA along the cerebral vasculature. (**A**, **B**) Aβ deposition in brain sections from control APP/PS1 and APP/PS1; n*Ext1*^{CKO} mice at 12 months of age was immunostained with a pan-Aβ antibody. Scale bar, 200 μm. (Inset) Immunostaining of Aβ deposition along leptomeningeal arteries as CAA in control APP/PS1 and APP/PS1; n*Ext1*^{CKO} mice. Scale bar, 10 μm. (**B**) The burden of CAA formation in leptomeningeal arteries in control APP/PS1 and APP/PS1; n*Ext1*^{CKO} mice (10 arteries/mouse; 10 mice/genotype) was quantified after scanning Aβ immunostaining by the Positive Pixel Count program (Aperio Technologies). Data represent mean ± SEM. $^{**}P < 0.01$. Statistical analysis was performed using Student's t test. (**C**) Co-immunofluorescence staining of leptomeningeal arteries with αSMA (green) and Aβ (red) antibodies. Scale bar, 10 μm.

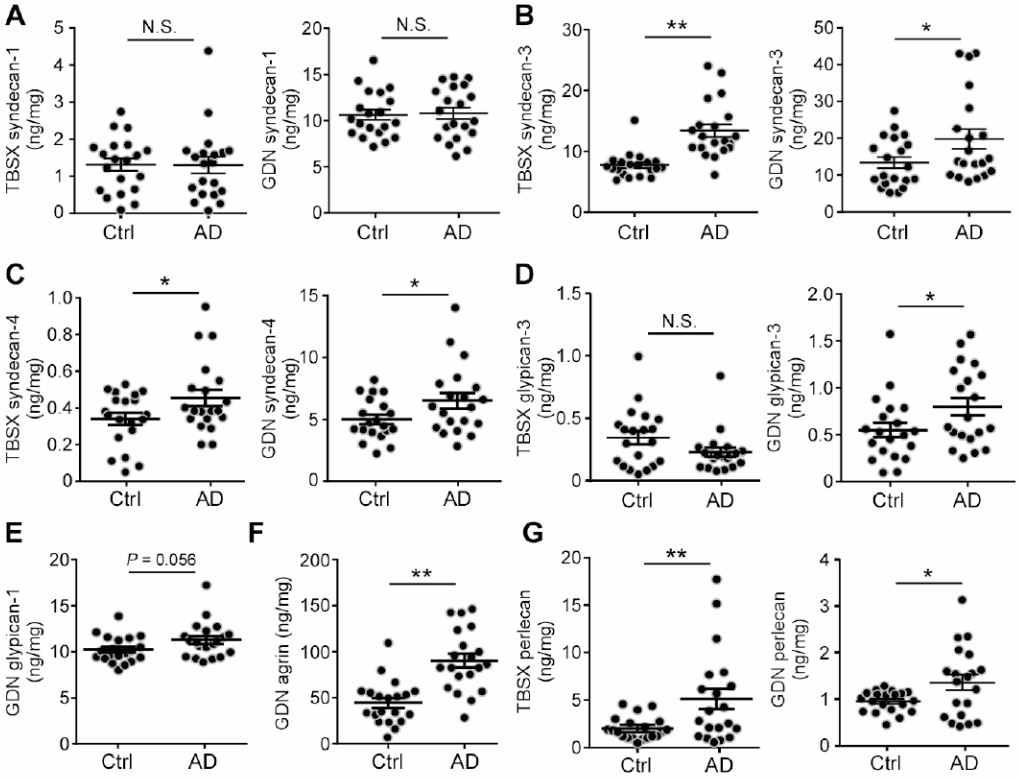

Fig. 5.

Several classes of HSPGs are elevated in human AD brain tissues. Human temporal lobe brain tissues from control (n=20) and AD (n=20) groups were lysed and fractionated through sequential extraction with TBS, TBSX, and GDN. (**A-C**) Transmembrane HSPGs, including syndecan-1, syndecan-3 and syndecan-4, in TBSX and GDN fractions of control and AD brain tissues were quantified by specific ELISAs. (**D**, **E**) The amounts of the GPI-anchored HSPGs glypican-1 and glypican-3 in TBSX and GDN fractions of control and AD brain tissue were quantified by specific ELISAs. (**F**, **G**) The amounts of two major extracellular matrix HSPGs agrin and perlecan in GDN fractions of control and AD brains were quantified by specific ELISAs. Results are presented as means ± SEM. N.S., not significant; *$P < 0.05$; **$P < 0.01$.